β-Ga2O3 HEMT for RF and High Power Nanoelectronics

Rajan Singh [1], Trupti Lenka [2], and Hieu Nguyen [1]

[1]Affiliation not available
[2]National Institute of Technology Silchar

October 30, 2023

Abstract

In this paper, we report record DC and RF performance in β-Ga_2O_3 High Electron Mobility Transistor (HEMT) with field-plate T-gate using 2-D simulations. The T gate with head-length L_{HL} of 180 nm and foot-length L_{FL} of 120 nm is used in the highly scaled device with an aspect ratio ($L_G/t_{barrier}$) of ~ 5. The proposed device takes advantage of a highly polarized Aluminum Nitride (AlN) barrier layer to achieve high Two-Dimensional Electron Gas (2DEG) density in the order of 2.3 × 10^{13} cm^{-2}, due to spontaneous as well as piezoelectric polarization components. In the depletion mode operation, maximum drain current $I_{D,MAX}$ of 1.32 A/mm, and relatively flat transconductance characteristics with a maximum value of 0.32 S/mm are measured. The device with source-drain distance L_{SD} of 1.9 μm exhibits record low specific-on resistance $R_{ON,sp}$ of 0.136 m-cm^{-2}, and off-state breakdown voltage of 403 V, which correspond to the record power figure-of-merit (PFoM) of ~ 1194 MW/cm^2. Additionally, current gain cut-off frequency f_T and maximum oscillation frequency f_{MAX} of 48 and 142 GHz are estimated. The obtained results show the potential of Ga_2O_3 HEMT for futuristic power devices.

T-Gate shaped AlN/β-Ga_2O_3 HEMT for RF and High Power Nanoelectronics

Rajan Singh
Department of Electronics and Communication Engineering,
National Institute of Technology Silchar,
Assam, India
Email: rajan_rs@ece.nits.ac.in

T. R. Lenka
Department of Electronics and Communication Engineering,
National Institute of Technology Silchar,
Assam, India
Email: trlenka@ieee.org

H. P. T. Nguyen
Department of Electrical and Computer Engineering,
New Jersey Institute of Technology Newark,
New Jersey, USA
Email: hieu.p.nguyen@njit.edu

***Abstract*—In this paper, we report record DC and RF performance in β-Ga_2O_3 High Electron Mobility Transistor (HEMT) with field-plate T-gate using 2-D simulations. The T gate with head-length L_{HL} of 180 nm and foot-length L_{FL} of 120 nm is used in the highly scaled device with an aspect ratio ($L_G/t_{barrier}$) of ~ 5. The proposed device takes advantage of a highly polarized Aluminum Nitride (AlN) barrier layer to achieve high Two-Dimensional Electron Gas (2DEG) density in the order of 2.3 × 10^{13} cm^{-2}, due to spontaneous as well as piezoelectric polarization components. In the depletion mode operation, maximum drain current $I_{D,MAX}$ of 1.32 A/mm, and relatively flat transconductance characteristics with a maximum value of 0.32 S/mm are measured. The device with source-drain distance L_{SD} of 1.9 µm exhibits record low specific-on resistance $R_{ON,sp}$ of 0.136 mΩ-cm^{-2}, and off-state breakdown voltage of 403 V, which correspond to the record power figure-of-merit (PFoM) of ~ 1194 MW/cm^2. Additionally, current gain cut-off frequency f_T and maximum oscillation frequency f_{MAX} of 48 and 142 GHz are estimated. The obtained results show the potential of Ga_2O_3 HEMT for futuristic power devices.**

Keywords—Beta-Gallium oxide (β-Ga_2O_3), High-Electron-Mobility-Transistor (HEMT), Power Figure-of-Merit (PFoM), T-Gate, Polarization, On-resistance (R_{ON}), Breakdown voltage (V_{BR}).

I. INTRODUCTION

Despite challenges on the front of high-quality native substrates, GaN-based HEMTs have been in use for over a decade and probably surpassed their life-cycle, for various reasons [1]. Currently, gallium-oxide (Ga_2O_3) is being thoroughly explored for its possible applications in certain areas of power electronics due to its interesting material properties such as large bandgap (4.5 - 5.3 eV), estimated high critical field (8 MV/cm), a wide variety of n-type dopants with controllable doping, and availability of single-crystal substrate grown using melt-based systems [2]–[4]. Out of its five crystalline structures, the β-phase of Ga_2O_3 has been reported as the most stable and looks most suited to high-voltage applications. The constant growth and development of β-Ga_2O_3 single crystal technology are further fuelling the search for a suitable wide-bandgap (WBG) material, having the potential to supplement existing technologies as well as capable to address new emerging power applications.

The β-Ga_2O_3 device technology has a footprint in almost all power devices including Schottky barrier diodes [5], [6], MESFETs [7], [8], MOSFETs: depletion-mode (D-mode) [9]–[12] and enhancement-mode (E-mode) [13]–[17], and HEMTs [18], [19]. Specifically, a high breakdown field of 3.8 and 5.2 MV/cm is reported in β-Ga_2O_3 lateral MOSFET [10] and β-Ga_2O_3 vertical heterostructure [20]. In addition, a power Figure of Merit (PFoM) $V_{BR}^2/R_{ON,sp}$ of 11 and 192.5 MW/cm^2 are reported in [10], and [17] respectively. However, these devices have used relatively thick epi-channel of 200 nm and large gate length of > 1µm together make them less relevant for RF applications. The high frequency applications demand aggressive device scaling, both lateral as well as vertical. On the other hand sub-micron gate led to poor control as well as deteriorated transconductance and current gain due to increased gate-resistance [21]. The T-gate technology enables use of short gate-length while keeping the gate-resistance low simultaneously [21]. It is worth to note that, the switching performance of a power switch critically depends on OFF-state leakage and ON-state conduction loss due to finite ON-resistance. Furthermore, the ON-resistance (R_{ON}) of the device is proportional to gate-drain length (L_{GD}) and sheet-resistance (R_{SH}) of the 2DEG channel.

In this paper, 2-D simulations of AlN/β-Ga_2O_3 HEMT are performed to access its switching performance using a physics-based device simulator. The DC and RF characteristics of the proposed device are thoroughly investigated. The following section describes the proposed device architecture and simulation settings, followed by results and discussion in Section III. Results are also benchmarked against similar device structure presented recently. Section IV concludes the paper.

II. DEVICE STRUCTURE AND SIMULATION FRAMEWORK

The proposed device schematic cross-section is shown in Fig. 1. The epitaxial layer sequence is arranged as follows. On a semi-insulating β-Ga_2O_3 substrate, 0.275 µm β-Ga_2O_3 buffer layer exists, which is doped with acceptor-like traps to account for unintentional Fe-dopants, followed by a 10 nm thick AlN material as a barrier layer on which Schottky gate contact with a barrier height of 0.8 eV is fixed. The source/drain contacts are assumed to be ohmic, and contact resistance of 0.4 Ω-mm is assumed as measured in [22]. The low contact resistance is achieved using a heavily doped n-type Gaussian profile with a peak concentration of 6 × 10^{19} cm^{-3}. The β-Ga_2O_3 material parameters and user-defined model parameters are mentioned at places where used, whereas the default physical models are used as given in [23]. The gate length, L_G equal to T-gate foot length (L_{FL}) of 120 nm and T-gate head length (L_{HL}) of 180 nm. The gate-source (L_{GS}) and gate-drain distance (L_{GD}) are equal to 0.32 and 1.4 µm respectively. Spontaneous and piezoelectric polarization models are evoked for the AlN barrier layer with default settings given in [23]. Apart from

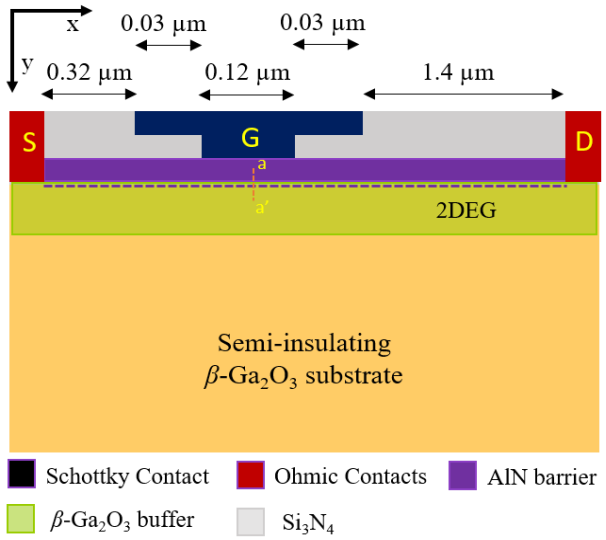

Fig. 1. Schematic of the investigated T-gate AlN/β-Ga_2O_3 HEMT, ohmic contacts access regions are n^+ doped (not shown here).

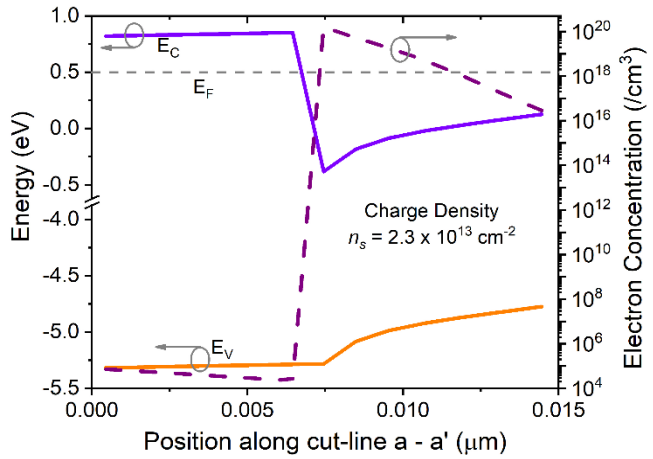

Fig. 2. Energy band diagram and electron concentration along the cut-line a – a' (shown in Fig. 1).

Shockley-Read-Hall (SRH) recombination, Fermi-Dirac for carrier statistics, electric field dependent mobility model—negative differential conductivity (NDC) is used to capture electron velocity saturation effect. To analyze breakdown characteristics, the impact ionization model—Selberherr is used.

The band bending and electron concentration at the heterointerface along the cut-line a – a' are shown in Fig. 2. The 2DEG density is estimated to be 2.3×10^{13} cm^{-2}. This high 2DEG density is attributed to high polarization charges confined in large conduction band offset (ΔE_C). The β-Ga_2O_3 material parameters such as energy bandgap E_G of 4.9 eV, static dielectric constant (ε_s) of 10.2 are taken from [24]. Using electron effective mass for conduction and valence band, total densities N_C and N_V of 3.6×10^{18} and 2.86×10^{20} cm^{-3} respectively, are used in the simulation deck. The β-Ga_2O_3 substrate is doped with acceptor as well as the donor-like trap of density 1×10^{18} cm^{-3} and at energy level 0.82, 4.4 eV respectively. Different β-Ga_2O_3 impact ionization coefficients for the Selberherr model [23] are taken from [25]. Electric field dependent mobility model NDC [26] is given as follows:

$$\mu_n(E) = \frac{\mu_0 + \frac{v_{sat}}{E}\left(\frac{E}{E_C}\right)^{\gamma}}{1+\left(\frac{E}{E_C}\right)^{\gamma}} \quad (1)$$

where v_{sat} = 1.5×10^7 cm/s is the saturation velocity, E_C = 200 kV/cm is the breakdown electric field, μ_0 = 140 cm^2/V s is the low-field electron mobility, and γ = 2.47 is the constant.

III. Results And Discussion

This section summarizes the numerical calculation of 2DEG density using polarization models, and simulation results of the T-gate AlN/β-Ga_2O_3 HEMT.

A. 2DEG Density

It is widely reported that a higher value of charge density (n_s) is critical for HEMTs operations since the current density is $\propto n_s$. Since β-Ga_2O_3 does not possess any polarization property, here only AlN barrier layer polarization is considered to calculate total sheet charge density. Total polarization $P_T = P_{SP} + P_{PI}$, where $P_{SP} = -0.09$ C/m^2 [23] is the spontaneous polarization of the AlN material. Due to tensile strain between AlN epitaxial layer and β-Ga_2O_3 buffer, piezoelectric polarization P_{PI} is given as:

$$P_{PI} = 2\left(\frac{a_s - a_0}{a_0}\right)e_{31} - \frac{C_{13}}{C_{33}}e_{33} \quad (2)$$

where a_s = 3.112, a_0 = 3.04 are the lattice constants of the AlN and β-Ga_2O_3 materials respectively, and piezoelectric constants are e_{31} = – 0.53, e_{33} = –1.5 C/m^2, and elastic constants are C_{13} = 127, C_{33} = 382 for AlN are used from [23]. So the total polarization P_T = – 0.612 C/m^2, which corresponds to sheet charge density $n_s \approx 3.8 \times 10^{14}$ cm^{-2}. However, this value is roughly one order greater than what is estimated through simulation. This can be attributed to the thickness-dependent piezoelectric polarization of the AlN barrier.

B. DC Characteristics

DC electrical transfer characteristics of the proposed device structure are shown in Fig. 3. The maximum value of drain current ($I_{D,MAX}$), and transconductance ($g_{M,MAX}$) are found to be 1.32 A/mm, 0.32 S/mm respectively at V_{GS} = 1V and V_{DS} = 12 V. A relatively 'flat' transconductance is obtained here and better device linearity can be expected. The improved g_m linearity is mainly due to the 'coupled' channel of the AlN barrier devices [27]. A threshold voltage (V_{TH}) of – 3.8 V at $I_D = I_{D,MAX}/10^3$, and I_{ON}/I_{OFF} greater than 10^7 are extracted from the log $I_D - V_{GS}$ curve, shown in Fig. 4. Output characteristics of the device, shown in Fig 5, are obtained at the different values of the V_{GS} varying from – 4 to 1 V in the step of 1 V. On-resistance (R_{ON}) is calculated corresponding to the linear part of the I_{DS}. The saturated drain current value of 1.35 A/mm is measured at V_{DS} = 12 V and V_{GS} = 1 V, which is almost equal to $I_{D,MAX}$.

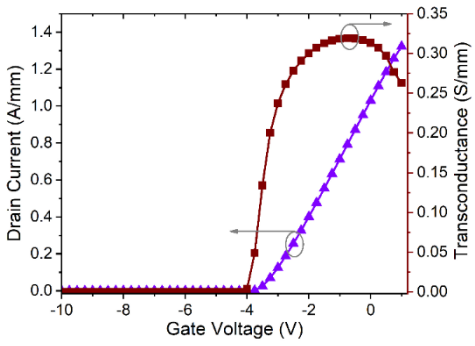

Fig. 3. Transfer characteristics (on a linear scale) of the AlN/β-Ga_2O_3 HEMT showing its transistor operation, V_{DS} = 12 V is used.

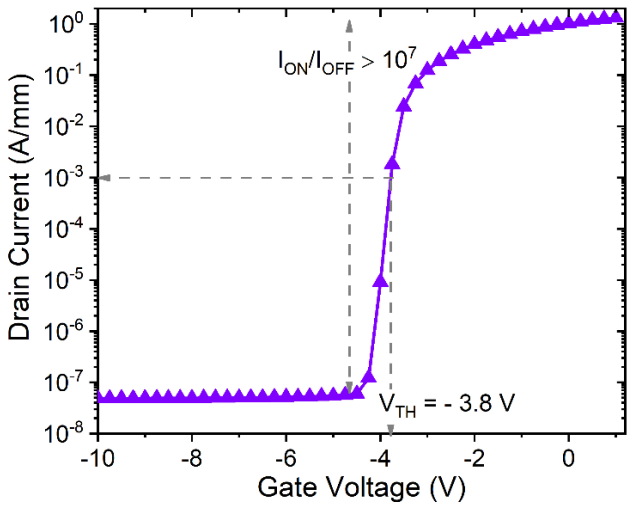

Fig. 4. Fig. 3. Transfer characteristics on log scale at V_{DS} = 12 V, showing $I_{ON}/I_{OFF} > 10^7$ and V_{TH} = – 3.8 V measured at V_{GS} where I_D is three orders lower than $I_{D,MAX}$.

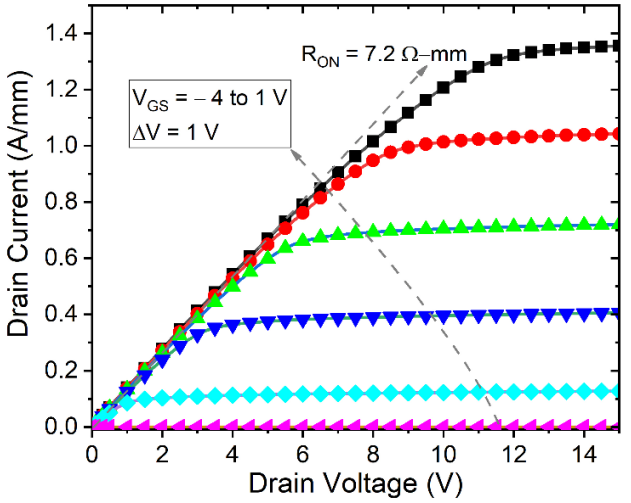

Fig. 5. Output characteristics of the AlN/β-Ga_2O_3 HEMT with L_G = 0.12 and L_{SD} = 1.9 µm, R_{ON} corresponding to linear part of I_{DS} is indicated.

On-resistance (R_{ON}) of 7.2 Ω-mm is extracted using the minimum of (V_{DS}/I_{DS}) at V_{GS} = 1 V in the simulation deck. The specific on-resistance ($R_{ON,sp}$) of the device is calculated as $R_{ON} \times L_{SD}$ = 0.136 mΩ-cm^2. The off-state breakdown voltage of the device is analysed using the Selberherr impact ionization model [23]. The default parameters of the model are replaced by β-Ga_2O_3 ionization coefficients (an1, an2 = 2.16 × 10^6, bn1 = bn2 = 1.77 × 10^7) reported in [25]. A minimum current density of 1 × 10^{-13} A is used in the simulation deck to trigger the breakdown. Since minority carriers are negligible in a wideband semiconductor like β-Ga_2O_3, numerical method—CLIMIT employed only one carrier—electrons. Compliance parameter is used to set current boundary conditions set at 1 mA/mm. The off-state breakdown voltage (V_{BR}) of the proposed structure with field-plate T-gate is estimated to be 403 V at V_{GS} = – 5V. The three-terminal breakdown characteristics are shown in Fig. 6. The peak electric field distribution at the breakdown is shown in Fig. 7. Moreover, the AlN/β-Ga_2O_3 HEMT with $R_{ON,sp}$ of 0.136 mΩ-cm^2 and V_{BR} of 403 V achieved a record power figure of merit (PFoM = $V_{BR}^2/R_{ON,sp}$) of 1194 MΩ/cm^2. This record value of PFoM supports the viability of AlN/β-Ga_2O_3 HEMT for high voltage Nanoelectronics applications.

C. RF Characteristics

The high-frequency RF performance of field-plate T-gate AlN/β-Ga_2O_3 HEMT is investigated to estimate current gain cutoff frequency (f_T) and maximum oscillation frequency (f_{MAX}). This part of the simulation is performed using a small signal analysis with ac frequency varying from 1 GHz to 200 GHz at V_{GS} = –1 V and V_{DS} = 12 V corresponding to g_m peak. Post simulation results show f_T of 68 GHz and f_{MAX} of 142 GHz and shown in Fig. 8. However, the estimated value of f_T is significantly lower than the previously reported f_T value by our group for AlN/β-Ga_2O_3 HEMT with gate-length L_G of 50 nm. Here, the lower f_T value can be explained based on the relatively large gate capacitance of T-gate as $f_T \propto 1/C_{GG}$, where C_{GG} is the gate capacitance, and also reported in [21].

D. Benchmarking

DC and RF parameters for the simulated AlN/β-Ga_2O_3 HEMT, along with similar devices reported recently, are provided in Table 1. The improved parameters are mainly due to the one-order higher 2DEG density (n_s) as compared to $n_s \approx 10^{12}$ cm^{-2} for delta-doped β-Ga_2O_3 MESFET [22]. In addition, a higher conduction band offset at the heterointerface ensures highly confined charge carriers in the quantum triangular well. Finally, the device is benchmarked in the $R_{ON,sp}$ versus V_{BR} plot along with other suitable reported devices, the respective plot is shown by Fig. 9.

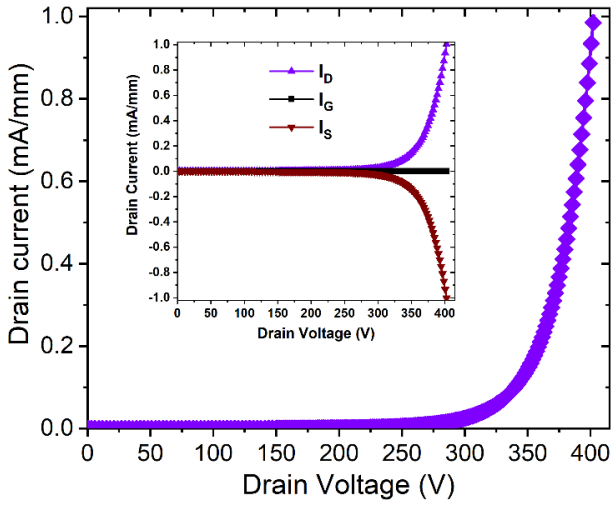

Fig. 6. Off-state breakdown characteristics of the AlN/β-Ga_2O_3 HEMT using field-plate T-gate with head length = 0.18 µm and foot length = 0.12 µm (= L_G). Inset: Three terminal breakdown characteristics. A V_{BR} of 403 V is estimated corresponding to I_{DS} = 1mA/mm.

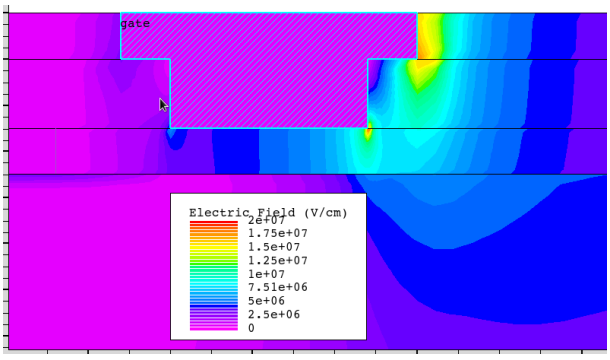

Fig. 7. Electric field profile (log scale) inside the simulated device structure at I_{DS} = 1 mA/mm, electric field peaks appear around drain side edges of field-plate T-gate.

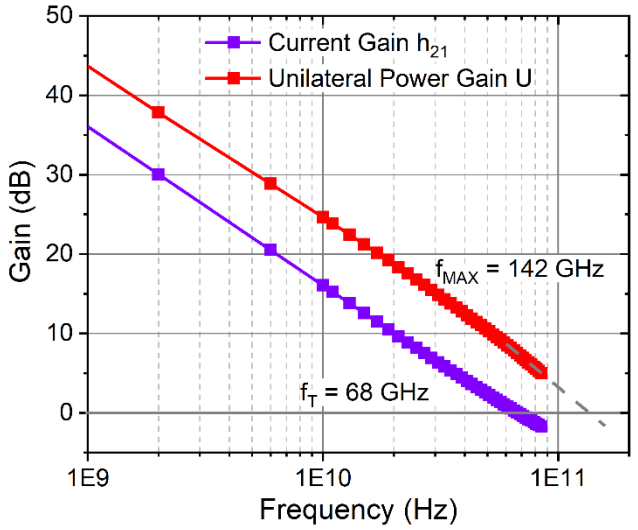

Fig. 8. Small-signal RF performance of AlN/β-Ga_2O_3 HEMT with field plate T-gate, DC operating point V_{DS} = 12 V, V_{GS} = – 1 V is applied.

Table 1. DC and RF parameters of field plate T-gate AlN/β-Ga_2O_3 HEMT and of T-gate β-Ga_2O_3 MESFET [22].

	Proposed device	Ref [22]
n_s (cm^{-2})	10^{13}	10^{12}
V_{TH} (V)	–3.8	–6
I_{ON}/I_{OFF}	10^7	10^8
$I_{D,MAX}$ (A/mm)	1.32	0.26
g_{MAX} (S/mm)	0.32	0.044
R_{ON} (Ω-mm)	7.2	–
$R_{ON,sp}$ (mΩ-cm^{-2})	0.136	–
f_T/f_{MAX} (GHz)	68/142	27/16

IV. Conclusion

In summary, DC and RF characteristics of AlN/β-Ga_2O_3 HEMT with field-plate T-gate are investigated via 2-D simulations. A high 2DEG density in the order of 10^{13} cm^{-2} is estimated at the heterointerface of AlN/β-Ga_2O_3 HEMT, mainly because of the highly polarized thin AlN barrier layer. Consequently, a maximum current density of 1.23 A/mm and peak transconductance of 0.32 S/mm are obtained. The proposed device employed a field plate T gate with head-length L_{HL} of 180 nm and foot-length L_{FL} of 120 nm to optimize its DC as well as RF performance. The T-gate effectively controls the channel and a threshold voltage of –3.8 V is estimated. The device has an ON-resistance of 7.2 Ω-mm, and a specific on-resistance of 0.136 mΩ-cm^2 corresponding to L_{SD} of 1.4 µm for the proposed device. Furthermore, using the impact ionization model and three-terminal breakdown characteristics, a breakdown voltage of 403 V is estimated, and combining $R_{ON,sp}$, and V_{BR}, a record PFoM of 1194 is estimated. The proposed device structure investigated here demonstrates the potential of AlN/β-Ga_2O_3 HEMTs for futuristic high-power Nanoelectronics applications.

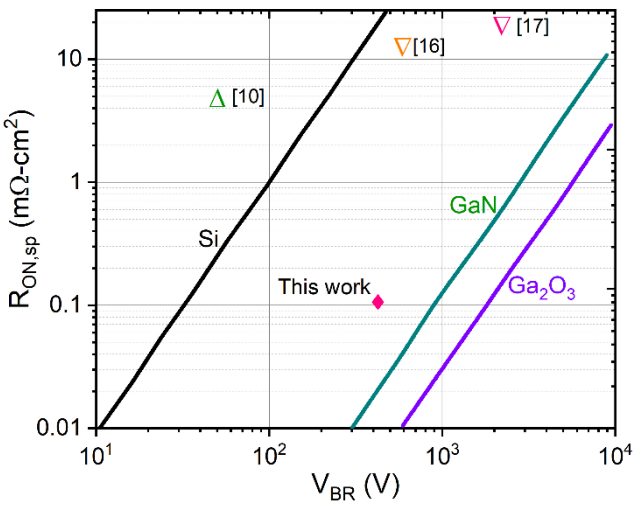

Fig. 9. $R_{ON,sp}$ versus V_{BR} for the field plate T gate AlN/βGa_2O_3 HEMT along with some other β-Ga_2O_3 devices. Data are shown relative to theoretical limits for Si, GaN and Ga_2O_3 materials.

Acknowledgement

Visvesvaraya Young Faculty Research Fellowship by Ministry of Electronics and Information Technology (MeitY), Govt. of India being implemented by Digital India Corporation.

References

[1] S. J. Pearton, F. Ren, M. Tadjer, and J. Kim, "Perspective: Ga_2O_3 for ultra-high power rectifiers and MOSFETS," J. Appl. Phys., vol. 124, no. 22, 2018, doi: 10.1063/1.5062841.

[2] S. J. Pearton et al., "A review of Ga_2O_3 materials, processing, and devices," Appl. Phys. Rev., vol. 5, no. 1, p. 011301, Mar. 2018, doi: 10.1063/1.5006941.

[3] E. Ahmadi and Y. Oshima, "Materials issues and devices of α- And β-Ga_2O_3," Journal of Applied Physics, vol. 126, no. 16. 2019, doi: 10.1063/1.5123213.

[4] R. Singh et al., "The dawn of Ga_2O_3 HEMTs for high power electronics - A review," Mater. Sci. Semicond. Process., vol. 119, no. September 2019, p. 105216, Nov. 2020, doi: 10.1016/j.mssp.2020.105216.

[5] Z. Hu et al., "Field-Plated Lateral β-Ga_2O_3 Schottky Barrier Diode with High Reverse Blocking Voltage of More Than 3 kV and High DC Power Figure-of-Merit of 500 MW/cm^2," IEEE Electron Device Lett., pp. 1–1, 2018, doi: 10.1109/LED.2018.2868444.

[6] J. Yang, F. Ren, M. Tadjer, S. J. Pearton, and A. Kuramata, "Ga_2O_3 Schottky rectifiers with 1 ampere forward current, 650 v reverse breakdown and 26.5 MW.cm^{-2} figure-of-merit," AIP Adv., vol. 8, no. 5, 2018, doi: 10.1063/1.5034444.

[7] M. Higashiwaki, K. Sasaki, A. Kuramata, T. Masui, and S. Yamakoshi, "Gallium oxide (Ga_2O_3) metal-semiconductor field-effect transistors on single-crystal β-Ga_2O_3 (010) substrates," Appl. Phys. Lett., vol. 100, no. 1, pp. 3–6, 2012, doi: 10.1063/1.3674287.

[8] S. Krishnamoorthy, Z. Xia, S. Bajaj, M. Brenner, and S. Rajan, "Delta-doped β-gallium oxide field-effect transistor," Appl. Phys. Express, vol. 10, no. 5, p. 051102, May 2017, doi: 10.7567/APEX.10.051102.

[9] M. Higashiwaki et al., "Depletion-mode Ga_2O_3 metal-oxide-semiconductor field-effect transistors on β-Ga_2O_3 (010) substrates and temperature dependence of their device characteristics," Appl. Phys. Lett., vol. 103, no. 12, pp. 1–5, 2013, doi: 10.1063/1.4821858.

[10] A. J. Green et al., "3.8-MV/cm Breakdown Strength of MOVPE-Grown Sn-Doped β-Ga_2O_3 MOSFETs," IEEE Electron Device Lett., vol. 37, no. 7, pp. 902–905, 2016, doi: 10.1109/LED.2016.2568139.

[11] N. Moser et al., "Ge-Doped β-Ga_2O_3 MOSFETs," IEEE Electron Device Lett., vol. 38, no. 6, pp. 775–778, Jun. 2017, doi: 10.1109/LED.2017.2697359.

[12] N. A. Moser et al., "High pulsed current density β-Ga_2O_3 MOSFETs verified by an analytical model corrected for interface charge," Appl. Phys. Lett., vol. 110, no. 14, p. 143505, Apr. 2017, doi: 10.1063/1.4979789.

[13] K. D. Chabak et al., "Enhancement-mode Ga_2O_3 wrap-gate fin field-effect transistors on native (100) β -Ga 2 O 3 substrate with high

breakdown voltage," Appl. Phys. Lett., vol. 109, no. 21, p. 213501, Nov. 2016, doi: 10.1063/1.4967931.

[14] M. H. Wong, Y. Nakata, A. Kuramata, S. Yamakoshi, and M. Higashiwaki, "Enhancement-mode Ga_2O_3 MOSFETs with Si-ion-implanted source and drain," Appl. Phys. Express, vol. 10, no. 4, p. 041101, Apr. 2017, doi: 10.7567/APEX.10.041101.

[15] T. Sato, K. Uryu, J. Okayasu, M. Kimishima, and T. K. Suzuki, "Suppression of drain-induced barrier lowering by double-recess overlapped gate structure in normally-off AlGaN-GaN MOSFETs," Appl. Phys. Lett., vol. 113, no. 6, pp. 2–6, 2018, doi: 10.1063/1.5039886.

[16] K. D. Chabak et al., "Recessed-Gate Enhancement-Mode β-Ga_2O_3 MOSFETs," IEEE Electron Device Lett., vol. 39, no. 1, pp. 67–70, Jan. 2018, doi: 10.1109/LED.2017.2779867.

[17] Z. Feng et al., "Design and fabrication of field-plated normally off β -Ga_2O_3 MOSFET with laminated-ferroelectric charge storage gate for high power application," Appl. Phys. Lett., vol. 116, no. 24, p. 243503, Jun. 2020, doi: 10.1063/5.0010561.

[18] J. Wang et al., "ε-Ga_2O_3: A Promising Candidate for High-Electron-Mobility Transistors," IEEE Electron Device Lett., vol. 41, no. 7, pp. 1052–1055, 2020, doi: 10.1109/LED.2020.2995446.

[19] R. Singh, T. R. Lenka, R. T. Velpula, B. Jain, H. Q. T. Bui, and H. P. T. Nguyen, "A novel β-Ga_2O_3 HEMT with fT of 166 GHz and X-band POUT of 2.91 W/mm," Int. J. Numer. Model. Electron. Networks, Devices Fields, vol. 34, no. 1, pp. 1–11, 2021, doi: 10.1002/jnm.2794.

[20] X. Yan, I. S. Esqueda, J. Ma, J. Tice, and H. Wang, "High breakdown electric field in β-Ga_2O_3/graphene vertical barristor heterostructure," Appl. Phys. Lett., vol. 112, no. 3, pp. 1–5, 2018, doi: 10.1063/1.5002138.

[21] J. Mateos, T. González, D. Pardo, V. Hoel, and A. Cappy, "Effect of the T-gate on the performance of recessed HEMTs. A Monte Carlo analysis," Semicond. Sci. Technol., vol. 14, no. 9, pp. 864–870, 1999, doi: 10.1088/0268-1242/14/9/320.

[22] Z. Xia et al., "β-Ga_2O_3 Delta-Doped Field-Effect Transistors With Current Gain Cutoff Frequency of 27 GHz," IEEE Electron Device Lett., vol. 40, no. 7, pp. 1052–1055, Jul. 2019, doi: 10.1109/LED.2019.2920366.

[23] D. S. Software, "ATLAS User ' s Manual," vol. II, no. November, pp. 567–1000, 2018.

[24] S. Poncé and F. Giustino, "Structural, electronic, elastic, power, and transport properties of β-Ga_2O_3 from first principles," Physical Review Research, vol. 2, no. 3. p. 033102, 2020, [Online]. Available: https://link.aps.org/doi/10.1103/PhysRevResearch.2.033102.

[25] K. Ghosh and U. Singisetti, "Impact ionization in β-Ga_2O_3," J. Appl. Phys., vol. 124, no. 8, p. 085707, Aug. 2018, doi: 10.1063/1.5034120.

[26] K. Ghosh and U. Singisetti, "Ab initio velocity-field curves in monoclinic β-Ga_2O_3," J. Appl. Phys., vol. 122, no. 3, p. 035702, Jul. 2017, doi: 10.1063/1.4986174.

[27] H. Lu, S. Member, B. Hou, L. Yang, X. Niu, and Z. Si, "AlN / GaN / InGaN Coupling-Channel HEMTs for Improved g m and Gain Linearity," pp. 1–6, 2021.